Inflammation Research (2020) 69:365–373
https://doi.org/10.1007/s00011-020-01331-3

Inflammation Research

ORIGINAL RESEARCH PAPER

Emodin alleviated pulmonary inflammation in rats with LPS-induced acute lung injury through inhibiting the mTOR/HIF-1α/VEGF signaling pathway

Xiaoqian Li[1,2] · Cong Shan[1,2] · Zhonghua Wu[1,2] · Hongji Yu[1,2] · Aidong Yang[1,2] · Bo Tan[3]

Received: 15 November 2019 / Revised: 10 February 2020 / Accepted: 25 February 2020 / Published online: 4 March 2020

Abstract

Objective and design This study aimed to investigate the anti-pulmonary inflammation effect of emodin on Wistar rats with lipopolysaccharide (LPS)-induced acute lung injury (ALI) and RAW264.7 cells through the mammalian target of rapamycin (mTOR)/hypoxia-inducible factor-1α (HIF-1α)/vascular endothelial growth factor (VEGF) signaling pathway.

Subjects Wistar rats and RAW264.7 cells were studied.

Treatment LPS was used to induce inflammation in rats or RAW264.7 cells and emodin was given once a day before LPS stimulation and continued for a certain number of days.

Methods Lung tissues and bronchoalveolar lavage fluid (BALF) were collected for the in vivo experiment, while cells and supernatant were collected for the in vitro experiment. Pathological changes in the lung tissues were assessed by hematoxylin and eosin staining. The levels of inflammatory factors, including TNF-α, IL-1β, and IL-6, were determined by enzyme-linked immunosorbent assay. The expression levels of p-mTOR, HIF-1α, and VEGF proteins were measured by Western blot analysis and immunohistochemistry. The mRNA levels of p70S6K, eIF4E-BP1, and eIF4E were measured by quantitative polymerase chain reaction.

Results Emodin ameliorated pathological changes and infiltrated inflammatory cells in LPS-induced ALI. It also significantly reduced the expression of inflammatory factors, including TNF-α, IL-1β, and IL-6, in BALF and downregulated the expression of p-mTOR, HIF-1α, and VEGF proteins in the lung tissues. Similar anti-inflammatory effects and the downregulation of the mTOR/HIF-1α/VEGF signaling pathway were found in RAW264.7 cells. The mRNA levels of p70S6K, eIF4E-BP1, and eIF4E also decreased in the macrophages.

Conclusion Emodin alleviated LPS-induced pulmonary inflammation in rat lung tissues and RAW264.7 cells through inhibiting the mTOR/HIF-1α/VEGF signaling pathway, which accounted for the therapeutic effects of emodin on ALI.

Keywords Acute lung injury · Emodin · mTOR/HIF-1α/VEGF signaling pathway · Pulmonary inflammation

Introduction

Acute lung injury (ALI) is the injury to alveolar epithelial cells and capillary endothelial cells induced by various direct and indirect factors, consequently inducing diffuse

Responsible Editor: John Di Battista.

Xiaoqian Li and Cong Shan contributed equally to this work.

✉ Aidong Yang
aidongy@126.com

✉ Bo Tan
tbot@163.com

[1] Research Centre on Application of Classical Prescriptions, Basic Medical College, Shanghai University of Traditional Chinese Medicine, Shanghai 201203, China

[2] Department of Febrile Disease, Basic Medical College, Shanghai University of Traditional Chinese Medicine, Shanghai 201203, China

[3] Clinical Pharmacokinetic Laboratory, Shuguang Hospital Affiliated to Shanghai University of Traditional Chinese Medicine, Shanghai 201203, China

pulmonary interstitial edema, alveolar edema, and acute or chronic hypoxic respiratory insufficiency. ALI and progressive acute respiratory distress syndrome are the major causes of acute respiratory failure, with the mortality rate as high as 30–40% [1]. Recent studies have shown that pulmonary edema and inflammatory infiltration, as well as hyperplasia of pulmonary microvascular endothelial cells induced by inflammatory factors, are important pathogeneses of ALI [2]. Therefore, efficient control of inflammatory responses is the key strategy for treating ALI.

Rheum officinale (Da Huang), a traditional Chinese medicine (TCM), could ameliorate inflammatory responses [3]. It has been used for treating pulmonary diseases in China over a thousand years [4]. Emodin is one of the major active components of *R. officinale*. It has various effects, including anti-inflammation, anti-tumor, and vasodilatation [5–7]. For example, emodin could reduce the expression of the nuclear transcription factor NF-κB and consequently control inflammatory responses during ALI [8, 9]. The mammalian target of the rapamycin (mTOR) signaling pathway participates in regulating biological activities of pulmonary vascular endothelium and alveolar epithelial cells during ALI and therefore plays an important role in the development and progression of ALI [10, 11]. The activation of the mTOR signaling pathway could potentially regulate the translocation of hypoxia-inducible factor-1α (HIF-1α) from the cytoplasm to the nuclei, which in turn improves the expression of vascular endothelial growth factor (VEGF), increases the infiltration of inflammatory factors, and aggravates ALI [11, 12]. However, only few studies have investigated the anti-inflammatory role of emodin in ALI through the mTOR/HIF-1α/VEGF signaling pathway.

In this study, rats with LPS-induced lung injury and RAW264.7 macrophages were used to investigate the role of the mTOR/HIF-1α/VEGF signaling pathway in the effects of emodin on alleviating inflammatory responses in ALI.

Materials and methods

Materials and regents

Emodin (98%; Sinopharm Chemical Reagent Co., Ltd, China), dexamethasone (DEX; 0.75 mg; Shanghai Xinyi Pharma Co., Ltd, China), endotoxin (LPS 055:B5, 057M4013V, Sigma, USA), rabbit multiclonal p-mTOR antibody (ab118815, Abcam, Cambridge, UK), rabbit multiclonal HIF-1α antibody (ab216842, Abcam), rabbit monoclonal VEGF antibody (ab32152, Abcam), anti-rabbit immunoglobulin G (H + L) (8889S, Cell Signaling, MA, USA), polyvinylidene difluoride (PVDF) membrane (Millipore, Bedford, MA, USA), enhanced chemiluminescence reagent (Beyotime Biotech, Jiangsu, China), EnVision reagent (HRP/Rabbit; Dako, Denmark), PrimeScript™ reverse transcription-polymerase chain reaction (RT-PCR) reagent kit with gDNA Eraser (TaKaRa, Kusatsu, Japan), and Opti-Minimum Eagle's medium (MEM) culture medium (Shanghai Universal Biotech Co, Shanghai, China) were used in this study. The primers for polymerase chain reaction (PCR) were synthesized by Invitrogen Ltd. (Shanghai) as follows according to a previous report: rat HIF1a, forward: 5′-GATGACGGCGACATGGTTTAC-3′, reverse: 5′-CTCACTGGGCCATTTCTGTGT-3′; rat eIF4E, forward: 5′-ACCCCTACCACTAATCCCCC-3′, reverse: 5′-CAATCGAAGGTTTGCTTGCCA-3′; rat Eif4ebp1, forward: 5′-GGGGACTACAGCACCACTC-3′, reverse: 5′-GTTCCGACACTCCATCAGAAAT-3′; rat p70S6K, forward: 5′-GGGGCTATGGAAAGGTTTTTCA-3′, reverse: 5′-CGTGTCCTTAGCATTCCTCACT-3′; rat GAPDH, forward: 5′-AGGTCGGTGTGAACGGATTTG-3′, reverse: 5′-TGTAGACCATGTAGTTGAGGTCA-3′.

Animals

Male Wistar rats ($n = 45$), with the age of 8 weeks and body weight of 180–220 g, were provided by the Experimental Animal Center of Shanghai University of Traditional Chinese Medicine (Certification No. SCXY(HU)2013–2016). The rats were kept in a controlled room (25 ± 2 °C, 45–60% humidity), with a cycle of 12-h light/12-h dark and allowed free access to food and water. They were randomly divided into five groups: normal group, model group (LPS only), dexamethasone (DEX) group, emodin low-dosage group (emodin-L group, 20 mg/kg), and emodin high-dosage group (emodin-H group, 40 mg/kg), with nine rats in each group. The corresponding drug was administered intragastrically for 5 days (once a day). LPS (8 mg/kg) was injected through the caudal vein 2 h after the gavage on the 5th day and then the samples were collected 7 h later. The emodin suspension was prepared using 0.5% sodium carboxymethylcellulose (CMC-Na) and the dosage volume was 10 mL/kg. For the rats in the normal and model groups, the same volume of CMC-Na was administered. For the rats in the DEX group, dexamethasone solution was given intragastrically with a dosage of 0.27 mg/kg. The use of the animals and the protocols of this study were approved by the Institutional Animal Care and Use Committee of Shanghai University of TCM (Animal Ethics Review No. SZY201708005). The study was conducted strictly in agreement with the China's laws of animal use and care.

Collection of bronchoalveolar lavage fluid and macrophages

The rats were anaesthetized by intraperitoneal injection of 20% urethan (5 mL/kg), and the bronchoalveolar lavage

fluid (BALF) was collected from the right lung. In brief, the bronchus in the right lung was exposed and then bronchial intubation was conducted. Normal saline with the total volume of 3 mL (4 °C, pH 7.0; 1 mL/time) was instilled, which was retrieved three times, and the recovery rate was > 90%. The BALF samples were centrifuged at 4 °C and 3000 rpm for 15 min and the supernatant was used for measuring the levels of inflammatory factors by enzyme-linked immunosorbent assay (ELISA). The precipitated cells were resuspended in Roswell Park Memorial Institute (RPMI) 1640 culture medium with 10% fetal bovine serum. A cell counting chamber was used to estimate the cell count and then the cell density was adjusted to 1×10^6/mL for further real-time PCR experiment.

Collection of lung tissues

After the BALF collection, those rats were sacrificed by cervical dislocation and the superior lobe of the right lung was harvested for pathological examinations and protein measurements. However, the left lung was washed with cold isotonic saline solution and blotted dry with a filter paper, then the wet weight (W) was measured. In addition, the right lung was placed in a 60 °C stove for 72 h and then the dry weight (D) was measured. The ratio of W/D was calculated.

Culture of RAW264.7 cells

The mouse macrophage cell line RAW264.7 was purchased from the Shanghai Cell Bank of the Chinese Academy of Sciences. The RAW264.7 cells were thawed and cultured with high-glucose full DMEM culture medium at 37 °C in the presence of 5% CO_2 in an incubator for 24 h and then the cells were observed under a microscope. After reaching 80–90% confluence, the cells were passaged. The macrophages in the logarithmic phase were collected for the experiments in this study. The cells were divided into six groups as following: normal group, model group (LPS only), emodin-L group (10 μM), emodin-M group (20 μM), and emodin-H group (40 μM), and rapamycin (RAPA) group (30 nmol/L). Cells with the density of 1×10^6/mL and 3 mL of DMEM culture medium were added to each well in the six-well culture plate and cultured for 18 h to allow the attachment of cells. Then, the culture medium was discarded, while emodin, RAPA, or blank CMC-Na solution were added to each group with a final concentration as designated above, respectively. After pre-treatment of 2 h, except for normal group LPS (final concentration of 500 ng/mL) was added to stimulate the cells for 16 h. Then, an inverted microscope was used to observe and record the cell morphology for all of the groups. Three replicates were used for each experimental group.

ELISA assay

ELISA kit was used to measure the levels of inflammatory factors, including TNF-α, IL-1β, and IL-6, in the BALF and supernatant of RAW264.7 cells, according to the manufacturers' protocols.

HE staining

The right superior lobe and intestine tissues were obtained and routinely fixed with 10% formaldehyde, followed by gradient dehydration. The samples were cut into small pieces measuring $1\times1\times0.3$ cm^3 for paraffin embedding, which was followed by slicing, bleaching, and HE staining. A light microscope was used to observe the pathological changes in the lung and intestinal tissues.

Immunohistochemistry assay

The paraffin-embedded slices were routinely dewaxed. Citrate buffer (CB), pH 6.0, was added for heat-induced antigen retrieval and then the slices were incubated with 0.3% H_2O_2 at room temperature for 20 min. Afterwards, 20% normal goat serum was added to incubate the slices for 30 min, the corresponding primary antibodies were added, and the slices were incubated at 37 °C for another 2 h. The slices were incubated with EnVision reagent (HPR/R) at 37 °C for 30 min, followed by development with diaminobenzidine (DAB) for 8–12 min, counterstained using hematoxylin, blow-dried, and then mounted with resin. The Image Analysis System for cell image analysis and Medical Image Analysis software were used to obtain the images and quantitatively analyze the data. Three individual visual fields were randomly selected for each slice. The ratio of the positive area in each sample was calculated (area of positive cells/total area) and used for the analysis. The pathological injuries of the lung tissues were assessed using the scoring criteria described by Kao [13].

Western blot analysis

Lung tissues or RAW264.7 cells were obtained and homogenized to extract the protein, which was quantified by the bicinchoninic acid (BCA) method. The same amount of protein was obtained for 6% SDS-PAGE electrophoresis, followed by constant voltage transmembrane at 100 V for 180 min. Then, the primary antibody (against p-mTOR, HIF-1α, or VEGF) was added and incubated at 4 °C overnight. The membrane was washed with TBST and then the diluted secondary antibody was added to incubate for 1 h. The membrane was washed with TBST again, following which the gel imaging analysis system was used for the analysis. The AlphaView SA software (ProteinSimple, CA,

USA) was used to analyze the grayscale value, which was used for the quantitative analysis. The ratio of the grayscale of the target strip to the grayscale of the strip of internal reference was calculated as the relative expression level of the target protein.

Real-time fluorescent PCR

A synthesis kit was used for the real-time fluorescent PCR following the manufacturers' protocols. Reverse transcription of 500 ng RNA was conducted to obtain the cDNA, with the reaction conditions as follows: 37 °C for 15 min, followed by 85 °C for 5 s. The conditions for the PCR were as follows: 95 °C for 30 s, followed by 95 °C for 3 s, and 60 °C for 30 s. The PCR was conducted for 40 cycles. The ΔCT method was used to assess the mRNA levels of the genes, using GAPDH as the internal reference.

Statistical analysis

All data were described with means and standard division. SPSS18.0 software (IBM, NY, USA) was used for the analysis of the data. One-way analysis of variance was conducted for the comparisons among different groups. $P < 0.05$ was considered statistically significant.

Results

Pathological changes in the lung tissues

The observations under the light microscope (200×) revealed interstitial pneumonia, interstitial microvascular edema, and inflammatory cell infiltration (++) in the model group (Fig. 1). However, the application of different concentrations of emodin evidently ameliorated the pathological changes in the lung tissues and the number of infiltrated inflammatory cells also decreased evidently (Fig. 1). The W/D ratio could better reflect the permeability of the interstitial capillaries and indicate the severity of pulmonary edema. The results in this study showed that compared with the normal group, the W/D ratio in the model group was significantly higher, while the application of emodin significantly reduced the W/D ratio (Fig. 1f).

Levels of TNF-α, IL-1β, and IL-6 in BALF and RAW264.7 cells

Compared with the normal group, the levels of TNF-α, IL-1β, and IL-6 proteins in BALF were significantly higher in the model group ($P < 0.05$). However, the levels of each

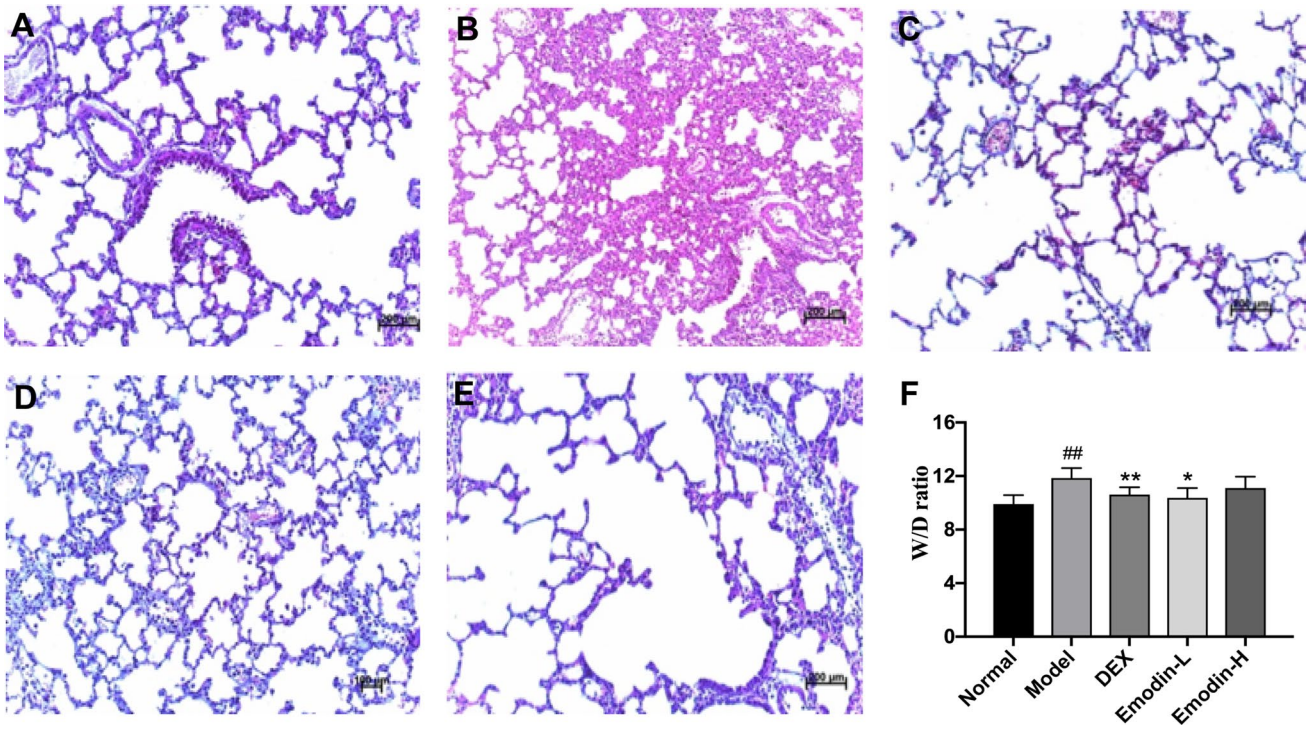

Fig. 1 Pathological changes in the lung tissues in rats. **a**–**e** Observing the slices of rat lung tissues under a light microscope (HE ×200). **a** Normal group; **b** model group (LPS only); **c** DEX group; **d** emodin-L group; **e** emodin-H group; and **f** wet weight vs dry weight (W/D) ratio of the lung tissues. $^{\#}P < 0.05$, compared with the normal group; $^{*}P < 0.05$, $^{**}P < 0.01$, compared with the model group

protein significantly decreased in the emodin-H group (Fig. 2a).

Regarding the results in the RAW264.7 cells, the levels of TNF-α, IL-1β, and IL-6 proteins increased significantly in the model group compared with the normal group ($P<0.05$ or $P<0.01$). The TNF-α level was significantly lower in the emodin-L, emodin-M, and RAPA groups than in the model group ($P<0.05$). IL-1β and IL-6 levels were also significantly lower in the emodin-M and RAPA groups than in the model group ($P<0.05$). In addition, the IL-6 level was significantly lower in the emodin-M group than in the RAPA group ($P<0.05$) (Fig. 2b).

Expression of mTOR, p-mTOR, HIF-1α, and VEGF in the lung tissues and RAW264.7 cells

Immunohistochemistry was adopted to assess the expression of mTOR, HIF-1α, and VEGF proteins in the lung tissues. The ratio of HIF-1α- or VEGF-positive area was significantly higher, while the mTOR expression was significantly lower, in the model group compared with the normal group (Fig. 3). However, compared with the model group, the ratio of the VEGF-positive area was significantly lower in the emodin-H group, the expression of mTOR was significantly higher in the emodin-H and emodin-L groups, and the expression of HIF-1α was significantly lower in the DEX group but significantly higher in the emodin-L group (Fig. 3). The western blot analysis showed that the expression of p-mTOR, HIF-1α, and VEGF was in agreement with the immunohistochemistry results. Compared with the normal group, the expression of p-mTOR, HIF-1α, and VEGF was significantly higher in the model group. However, the application of emodin significantly reduced the expression of p-mTOR, HIF-1α, and VEGF proteins in a concentration-dependent manner (Fig. 4).

Western blot analysis in RAW264.7 cells showed that the expression of p-mTOR, HIF-1α, and VEGF proteins was significantly higher in the model group than in the normal

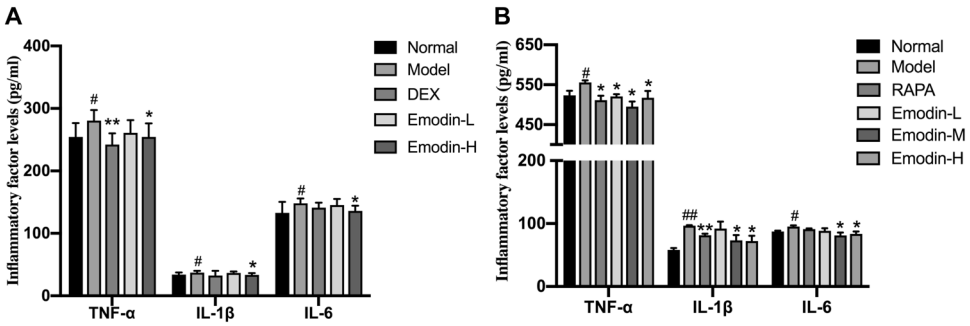

Fig. 2 Levels of TNF-α, IL-1β, and IL-6 (pg/mL) in the bronchoalveolar lavage fluid in rats (**a**, $n=9$) and RAW264.7 cells (**b**, $n=3$). $^{\#}P<0.05$, compared with the normal group; $^{*}P<0.05$, $^{**}P<0.01$, compared with the model group (LPS only)

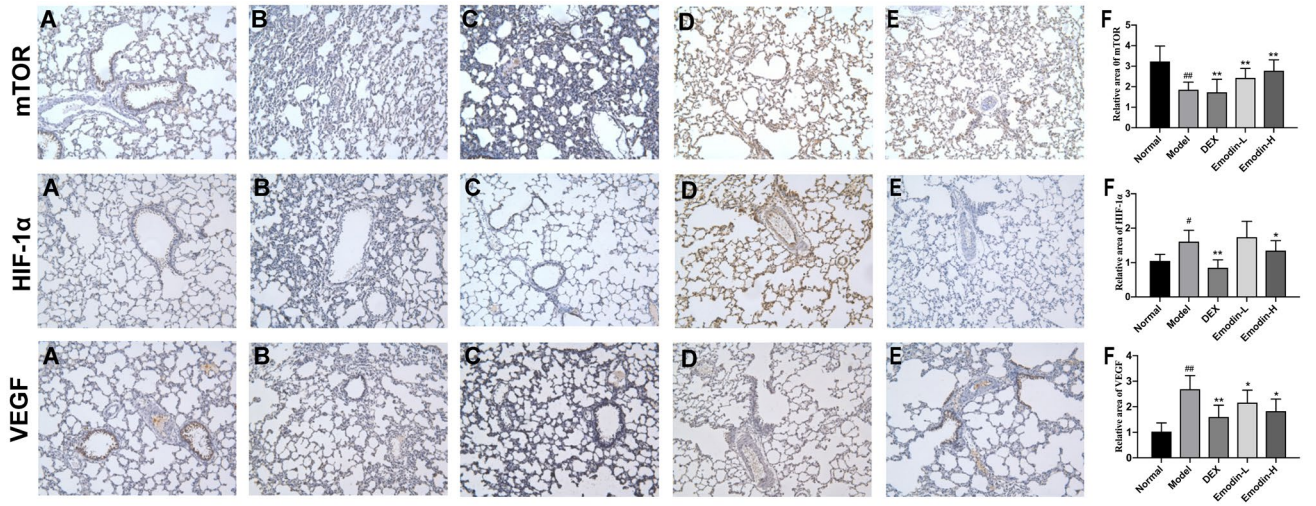

Fig. 3 Expression of mTOR, HIF-1α, and VEGF proteins in the lung tissues in rats (immunohistochemistry, ×200). **a** Normal group; **b** model group (LPS only); **c** DEX group; **d** emodin-L group; **e** emodin-H group; **f** the relative area of positive stain for each protein. The observation under the microscope showed that the background was purple-blue, while the positive proteins were stained brown-yellow or yellow. $^{\#}P<0.05$, compared with the normal group; $^{*}P<0.05$, $^{**}P<0.01$, compared with the model group

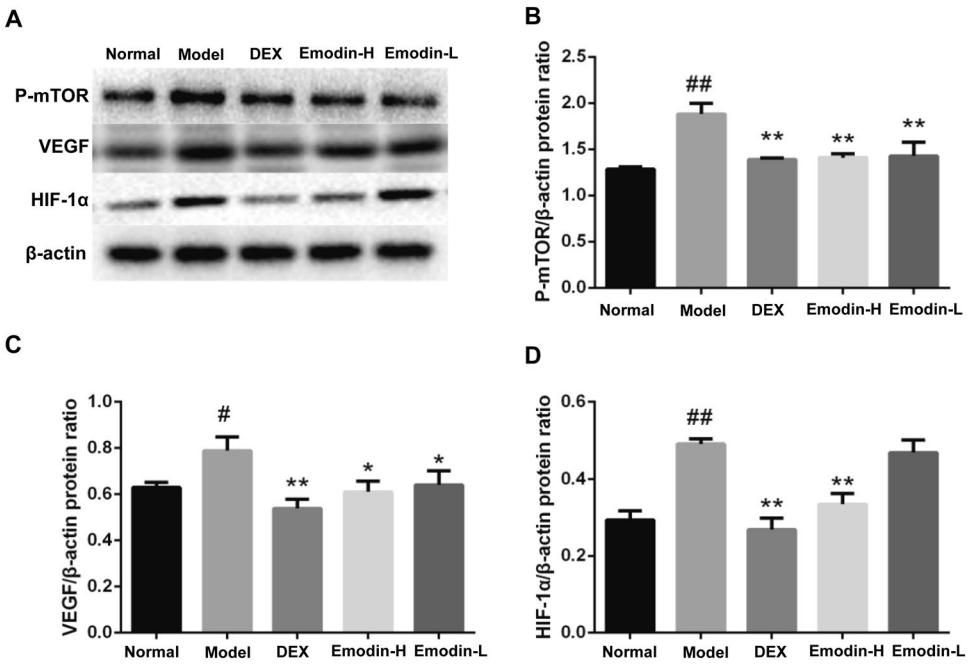

Fig. 4 Expression of p-mTOR, HIF-1α, and VEGF proteins in the lung tissues in rats. Representative western blots (**a**) and quantitative analysis for p-mTOR (**b**), VEGF (**c**), and HIF-1α (**d**) protein expression. $^{\#}P<0.05$, compared with the normal group; $^{*}P<0.05$, $^{**}P<0.01$, compared with the model group (LPS only)

group ($P<0.01$). In addition, compared with the model group, the expression of p-mTOR, HIF-1α, and VEGF proteins was significantly lower in the emodin-H, emodin-M, and emodin-L groups. Furthermore, in all dosages of emodin groups, the expression of p-mTOR, HIF-1α, and VEGF proteins showed similar tendency with that in RAPA group, which received a specific mTOR inhibitor (Fig. 5).

Expression of p70S6K, eIF4E-BP1, and eIF4E mRNA in BALF macrophages and RAW264.7 cells

Compared with the normal group, the expression of p70S6K, eIF4E-BP1, and eIF4E mRNA in BALF macrophages was significantly higher in the model group. In addition, compared with the model group, the expression of p70S6K,

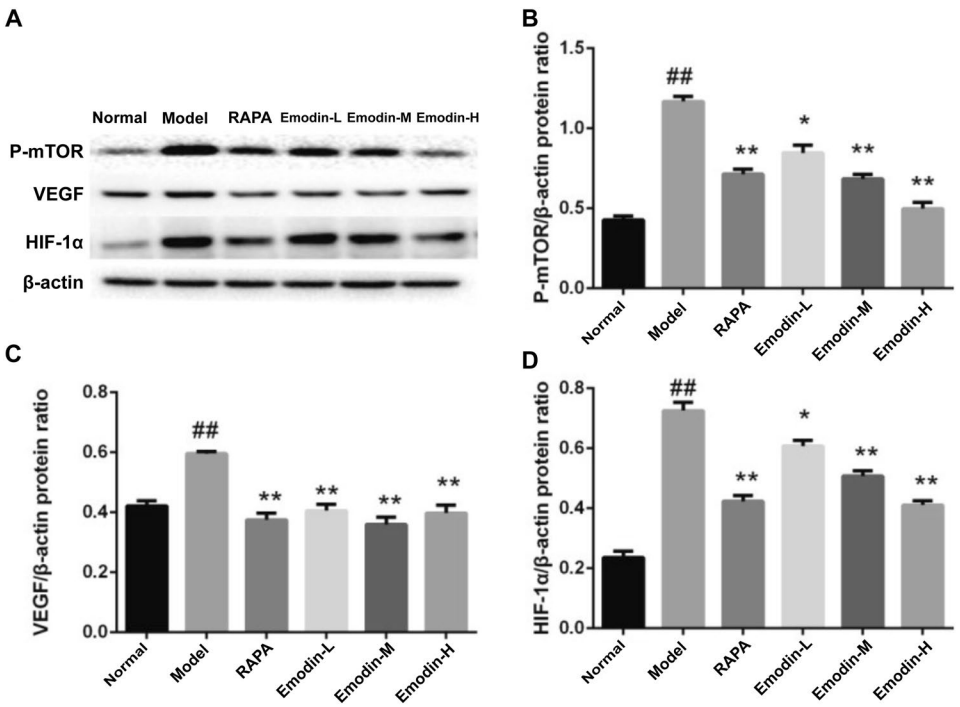

Fig. 5 Expression of p-mTOR, HIF-1α, and VEGF proteins in RAW264.7 cells. Representative western blots (**a**) and quantitative analysis for p-mTOR (**b**), VEGF (**c**), and HIF-1α (**d**) protein expression. $^{\#}P<0.05$, compared with the normal group; $^{*}P<0.05$, $^{**}P<0.01$, compared with the model group (LPS only)

eIF4E-BP1, and eIF4E mRNA decreased significantly after the application of emodin (Fig. 6a).

Compared with the normal group, the expression of p70S6K, eIF4E-BP1, and eIF4E mRNA in RAW264.7 cells was significantly higher in the model group. However, compared with the model group, HIF-1α mRNA was significantly higher in the emodin-L group, p70S6K mRNA was significantly lower in the emodin-L and emodin-M groups, eIF4E-BP1 mRNA was significantly lower in the emodin-L group, and eIF4E mRNA was significantly lower in the emodin-L and emodin-M groups (Fig. 6b).

Discussion

The pathogeneses of ALI are complex and the pathological bases of ALI are associated with pulmonary capillary membrane injuries, pulmonary edema, and hyaline membrane formation, which are induced by the uncontrolled pulmonary inflammatory responses [2, 14]. LPS, a type of endotoxin, stimulates the release of various inflammatory mediators and is an important factor inducing ALI. The HIF-1α/VEGF signaling pathway plays an important role in the pathogeneses of ALI and pulmonary edema [15, 16]. Upon hypoxia, HIF-1α induces and activates the overexpression of *VEGF* gene [17–19], which consequently promotes the division of vascular endothelial cells, induces angiogenesis, and increases vascular permeability. This results in hypertonic pulmonary edema and injuries to pulmonary capillary endothelial cells in ALI [20]. Inhibiting HIF-1α-induced inflammatory responses in macrophages could help reduce inflammation-associated tissue injuries. The mTOR signaling pathway is associated with various events, such as cell differentiation and proliferation. The phosphorylation of mTOR could regulate the phosphorylation of various transcription factors, including p70S6K and 4E-BP1, while the phosphorylation of p70S6K could further promote the expression of HIF-1α [21]. In addition, the phosphorylation of 4E-BP1 could also promote the release of mRNA cap-binding protein eIF4E and induce the phosphorylation and consequent translation of HIF-1α and other proteins [20]. However, the regulatory effects of the mTOR signaling pathway on HIF-lα and VEGF are still controversial [22]. The regulatory effects of mTOR on HIF-lα and VEGF vary in different microenvironments or cell lines, while the roles of this pathway in ALI are still unclear. The present study found that the phosphorylation of mTOR in macrophages increased significantly in in vivo and in vitro models, which was accompanied by the upregulation of HIF-1α and VEGF. After the application of mTOR inhibitor RAPA, the expression of HIF-1α and VEGF in macrophages decreased, which was in agreement with previous findings [23]. These findings demonstrated that the mTOR/HIF-1α/VEGF signaling pathway in the lung tissues of rat models of LPS-induced ALI was activated.

TCM documented *R. officinale* as a drug that could be used to purge heat, clear intestine, cool blood, detoxify, remove stagnation, unblock meridian, and improve the respiratory functions in ALI [24, 25]. Emodin is the major active component of *R. officinale*. Several previous studies demonstrated that emodin could inhibit the inflammatory responses and regulate pulmonary water metabolism, anti-oxidation, and expression of pulmonary surfactant-related proteins during ALI [9, 26, 27]. This study showed that emodin could significantly reduce the expression of p-mTOR; decrease the levels of inflammatory factors such as TNF-α, IL-1β, and IL-6 in BALF; and downregulate the mRNA expression of various transcription factors, including p70S6K, eIF4E-BP1, and eIF4E. Therefore, it was hypothesized that emodin could inhibit the phosphorylation of mTOR, consequently downregulate the downstream mRNA expression of p70S6K and eIF4E, inhibit the expression of HIF-1α and downstream the *VEGF* gene [28], and thereby inhibit the release of inflammatory factors and improve ALI. However, the findings in RAW264.7 cells showed that the level of HIF-1α did not decrease significantly in the emodin-L and emodin-M groups, while the levels of p70S6K and eIF4E mRNA decreased significantly, which could be associated with the effects of emodin on the half-life of HIF-1α protein [29].

In summary, the findings of this study demonstrated that the activation of the mTOR/HIF-1α/VEGF pathway was

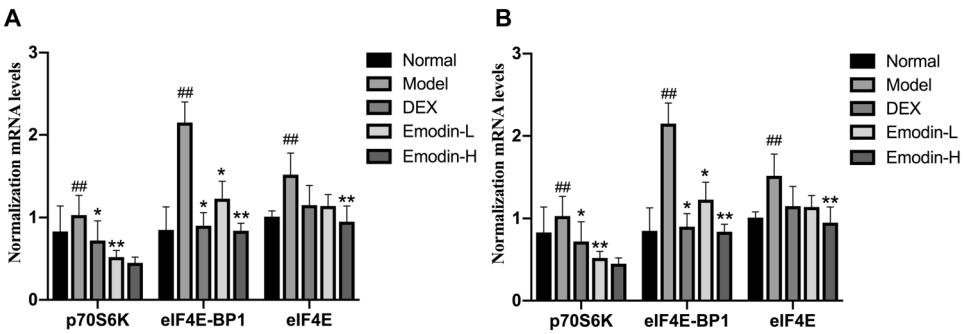

Fig. 6 Comparison of HIF-1α, p70S6K, IF4E-BP1, and eIF4E mRNA levels in the bronchoalveolar lavage fluid in rats (**a**, $n=9$) and RAW264.7 cells (**b**, $n=3$). $^{\#}P<0.05$, compared with the normal group; $^{*}P<0.05$, $^{**}P<0.01$, compared with the model group (LPS only)

associated with the inflammatory responses in ALI, while inhibiting this pathway could ameliorate the inflammatory responses in ALI. Emodin could inhibit the mTOR/HIF-1α/VEGF pathway, which could be one of the potential mechanisms involved in the therapeutic effects of *R. officinale* on ALI.

Acknowledgements This study was supported by the National Natural Science Foundation of China (81673855), the Ministry of Science and Technology of China (2018YFC1704100, 2017ZX09304002), the Shanghai Municipal Health Committee (ZY(2018-2020)-CCCX-2001-01, 201740199), the Shanghai University of TCM (A1-Z193020109), and the Shanghai Shuguang Hospital (SGXZ-201907).

Author contributions XQL, ADY, and BT conceived the study design, collected and analyzed the data, and wrote the manuscript. CS, ZHW, and HJY performed the animal experiments. Molecular biological studies were performed by XQL, ZHW, and HJY. CS, ADY, and BT contributed substantially to collecting and interpreting the data. All authors read and approved the final manuscript.

Compliance with ethical standards

Conflict of interest The authors declare no conflicts of interest.

References

1. Matthay MA, Zemans RL, Zimmerman GA, Arabi YM, Beitler JR, Mercat A, et al. Acute respiratory distress syndrome. Nat Rev Dis Primers. 2019;5(1):18.
2. Levy BD, Serhan CN. Resolution of acute inflammation in the lung. Annu Rev Physiol. 2014;76:467–92.
3. Song G, Zhang Y, Yu S, Lv W, Guan Z, Sun M, et al. Chrysophanol attenuates airway inflammation and remodeling through nuclear factor-kappa B signaling pathway in asthma. Phytother Res. 2019;33(10):2702–13.
4. Chang G. Discussion on the effect of Rhubarb in the treatment of children whit pulmonary disease. Chin Pediatr Integr Tradit West Med. 2019;11.
5. Wu L, Cai B, Zheng S, Liu X, Cai H, Li H. Effect of emodin on endoplasmic reticulum stress in rats with severe acute pancreatitis. Inflammation. 2013;36(5):1020–9.
6. Hwang JK, Noh EM, Moon SJ, Kim JM, Kwon KB, Park BH, et al. Emodin suppresses inflammatory responses and joint destruction in collagen-induced arthritic mice. Rheumatology (Oxford). 2013;52(9):1583–91.
7. Song YD, Li XZ, Wu YX, Shen Y, Liu FF, Gao PP, et al. Emodin alleviates alternatively activated macrophage and asthmatic airway inflammation in a murine asthma model. Acta Pharmacol Sin. 2018;39(8):1317–25.
8. Zhang W, Lu X, Wang W, Ding Z, Fu Y, Zhou X, et al. Inhibitory effects of emodin, thymol, and astragalin on leptospira interrogans-induced inflammatory response in the uterine and endometrium epithelial cells of mice. Inflammation. 2017;40(2):666–75.
9. Xiao M, Zhu T, Zhang W, Wang T, Shen YC, Wan QF, et al. Emodin ameliorates LPS-induced acute lung injury, involving the inactivation of NF-kappaB in mice. Int J Mol Sci. 2014;15(11):19355–68.
10. Üstün S, Lassnig C, Preitschopf A, Mikula M, Müller M, Hengstschläger M, et al. Effects of the mTOR inhibitor everolimus and the PI3K/mTOR inhibitor NVP-BEZ235 in murine acute lung injury models. Transpl Immunol. 2015;33(1):45–50.
11. Hu Y, Liu J, Wu YF, Lou J, Mao YY, Shen HH, et al. mTOR and autophagy in regulation of acute lung injury: a review and perspective. Microbes Infect. 2014;16(9):727–34.
12. Karmpaliotis D, Kosmidou I, Ingenito EP, Hong K, Malhotra A, Sunday ME, et al. Angiogenic growth factors in the pathophysiology of a murine model of acute lung injury. Am J Physiol Lung Cell Mol Physiol. 2002;283(3):L585–L595595.
13. Kao SJ, Wang D, Yeh DY, Hsu K, Hsu YH, Chen HI. Static inflation attenuates ischemia/reperfusion injury in an isolated rat lung in situ. Chest. 2004;126(2):552–8.
14. Butt Y, Kurdowska A, Allen TC. Acute lung injury: a clinical and molecular review. Arch Pathol Lab Med. 2016;140(4):345–50.
15. McClendon J, Jansing NL, Redente EF, Gandjeva A, Ito Y, Colgan SP, et al. Hypoxia-inducible factor 1alpha signaling promotes repair of the alveolar epithelium after acute lung injury. Am J Pathol. 2017;187(8):1772–866.
16. Jiang H, Huang Y, Xu H, Hu R, Li QF. Inhibition of hypoxia inducible factor-1alpha ameliorates lung injury induced by trauma and hemorrhagic shock in rats. Acta Pharmacol Sin. 2012;33(5):635–43.
17. Yuan G, Nanduri J, Khan S, Semenza GL, Prabhakar NR. Induction of HIF-1alpha expression by intermittent hypoxia: involvement of NADPH oxidase, Ca^{2+} signaling, prolyl hydroxylases, and mTOR. J Cell Physiol. 2008;217(3):674–85.
18. Lin F, Pan LH, Ruan L, Qian W, Liang R, Ge WY, et al. Differential expression of HIF-1alpha, AQP-1, and VEGF under acute hypoxic conditions in the non-ventilated lung of a one-lung ventilation rat model. Life Sci. 2015;124:50–5.
19. Yamazaki Y, Egawa K, Nose K, Kunimoto S, Takeuchi T. HIF-1-dependent VEGF reporter gene assay by a stable transformant of CHO cells. Biol Pharm Bull. 2003;26(4):417–20.
20. Zhang X, Li J, Li C, Li Y, Zhu W, Zhou H, et al. HSPA12B attenuates acute lung injury during endotoxemia in mice. Int Immunopharmacol. 2015;29(2):599–606.
21. Bian CX, Shi Z, Meng Q, Jiang Y, Liu LZ, Jiang BH. P70S6K 1 regulation of angiogenesis through VEGF and HIF-1alpha expression. Biochem Biophys Res Commun. 2010;398(3):395–9.
22. Brugarolas JB, Vazquez F, Reddy A, Sellers WR, Kaelin WG. TSC2 regulates VEGF through mTOR-dependent and -independent pathways. Cancer Cell. 2003;4(2):147–58.
23. Jo YY, Kim DW, Choi JY, Kim SG. 4-Hexylresorcinol and silk sericin increase the expression of vascular endothelial growth factor via different pathways. Sci Rep. 2019;9(1):3448.
24. Li C, Zhou J, Gui P, He X. Protective effect of rhubarb on endotoxin-induced acute lung injury. J Tradit Chin Med. 2001;21(1):54–8.
25. Li WY, Chan SW, Guo DJ, Chung MK, Leung TY, Yu PH. Water extract of *Rheum officinale* Baill. induces apoptosis in human lung adenocarcinoma A549 and human breast cancer MCF-7 cell lines. J Ethnopharmacol. 2009;124(2):251–6.
26. Zhu T, Zhang W, Feng SJ, Yu HP. Emodin suppresses LPS-induced inflammation in RAW264.7 cells through a PPARgamma-dependent pathway. Int Immunopharmacol. 2016;34:16–24.
27. Cui H, Li S, Xu C, Zhang J, Sun Z, Chen H. Emodin alleviates severe acute pancreatitis-associated acute lung injury by decreasing pre-B-cell colony-enhancing factor expression and promoting polymorphonuclear neutrophil apoptosis. Mol Med Rep. 2017;16(4):5121–8.

28. Zhang EY, Gao B, Shi HL, Huang LF, Yang L, Wu XJ, et al. 20(S)-Protopanaxadiol enhances angiogenesis via HIF-1alpha-mediated VEGF secretion by activating p70S6 kinase and benefits wound healing in genetically diabetic mice. Exp Mol Med. 2017;49(10):e387.
29. Liu YN, Pan SL, Liao CH, Huang DY, Guh JH, Peng CY, et al. Evodiamine represses hypoxia-induced inflammatory proteins expression and hypoxia-inducible factor 1alpha accumulation in RAW264.7. Shock. 2009;32(3):263–9.